



# The Effect of Sunglint on Satellite-Based Benthic Habitat Identification

Pramaditya Wicaksono

Cartography and Remote Sensing, Faculty of Geography,  
Universitas Gadjah Mada Yogyakarta 55281, Indonesia

**Abstract** — *Benthic habitat mapping using high spatial resolution image exhibits several issues. One of the issues is the occurrence of sunglint on water surface which alter intra habitat spectral variation recorded by the sensor. Prior to further image analysis, sunglint should be removed to avoid any spectral and radiometric confusion. This study aimed at removing sunglint from Quickbird image and analyzes the effect of sunglint on altering benthic habitat spectral variation. Infrared (IR) band was used to normalize the variation of sunglint on visible bands. In order to analyze habitat's spectral variation due to sunglint, coefficient of variation analysis was performed on raw and corrected Quickbird image. The results showed that NIR band was very effective to remove sunglint from visible bands. In addition, we found out that an average of 64.3% variation within particular habitat class was due to sunglint. Furthermore, we also found that sunglint correction reveals inherent information about benthic habitat that has been previously covered by sunglint.*

**Keywords**— *benthic habitat, Quickbird, sunglint, coefficient of variation*

## I. INTRODUCTION

Remote sensing technology is highly suitable for replacing the extensive field survey of benthic habitat mapping and put the information about benthic habitat in spatial and temporal context. Remote sensing has the ability to cover large portion of earth, identifies object's spectral information, and temporally records data at various spatial resolutions. Remote sensing for benthic habitat mapping requires visible bands with its water penetration ability. Visible bands have the ability to penetrate water up to 25 m when the water is very clear [4]. However, the maximum penetration ability varies with geographical and water condition [16]. However, visible bands have lower penetration ability when interacted with more turbid water due to the scattering performed by the sediment suspended on water column. Ideally, wavelengths longer than NIR should not be used for identifying underwater objects because those ranges of energies are effectively absorbed by water. Consequently, they cannot penetrate into water body, and thus produce very low reflectance and appear dark on the image.

Remote sensing images equipped with the ability to perform underwater mapping are Landsat series ([2], [14]), SPOT series ([13], [25]), ASTER VNIR [17], ALOS AVNIR-2 [22], IKONOS ([1], [21]), Quickbird ([10], [23]), Geoeye-1, Worldview-2, and Rapideye. Those images are multispectral and have the ability to effectively map benthic habitat up to the second level of detail at [18] benthic habitat classification scheme [16]. Beyond the second level of the scheme or going

into life-form and species level is quite difficult for those images. Currently, the best image for benthic habitat mapping is the hyperspectral ([7], [15], [23]). Hyperspectral data such as CASI manages to perform well until the third level of benthic habitat hierarchical classification scheme. Despite the performance for benthic habitat mapping, CASI as well as other hyperspectral data are not widely available. Since the platform of most hyperspectral sensor is airborne, the operational cost is high, the area coverage is small, and the processing technique is more complex than multispectral image. Therefore, the selection of remote sensing data used to perform benthic habitat mapping is highly depends on the purpose of the mapping and the required level of detail of the output map.

Remote sensing is very promising on replacing the extensive field survey of benthic habitat. However, remote sensing of benthic habitat mapping poses sunglint issue due to the overlying water surface. Sunlight is a specular reflection occurs in water surface caused by wind-driven wave. Sunlight occurs on the waves crest and produces a circular bright band that obscures the underlying information. Furthermore, the occurrence of sunglint may worsen when the sensor viewing angle is relatively similar with the angle of sunlight reflected off the water surface. Even though sunglint can be useful to interpret wind direction, surface water currents, oil slick, and water temperature [8], it is quite a problem for underwater mapping activities. In short, in spite of its promising capacity, remote sensing for underwater mapping is still affected by sunglint issue.

Sunglint acutely occurs on the condition where remote sensing performs optimally for underwater mapping. Sunglint appears when the cloud coverage is minimal, the water is optically shallow and clear, and the image is recorded at high spatial resolution. The existence of sunglint is unfortunate because at this optimal condition, remote sensing image is expected to deliver optimum information about benthic habitat. Consequently, in order to optimally using remote sensing images for benthic habitat mapping, sunglint should be removed prior to further image analysis.

This study covers the removal of sunglint on Quickbird image as well as the comparison analysis between the original image and sunglint-free image. That analysis was intended to see how much sunglint alters benthic habitat spectral information. High spatial and radiometric resolution data such as Quickbird was selected because the appearance of sunglint on such kind of data is more prominent than in medium or coarse resolution data. At lower resolution, sunglint is partly generalized by the large pixel size and low data digitization. Therefore, the impact of sunglint removal is also more evident at higher resolution data.

Furthermore, Coefficient of Variation (COV) analysis was used to see how the information within particular class habitat is altered due to sunglint effect. The method to remove sunglint from Quickbird image was developed by [11]. The method utilizes IR band for correcting the sunglint in the available visible bands.

## II. STUDY AREA AND IMAGE DATA

The study area was located within the National Park of Ujung Kulon. The area is administratively located on Kecamatan Sumur and Cimanggu, Pandeglang District, Banten Province. The whole National Park is extending from 102° 2' 32" E to 102° 37' 37" E and 6° 30' 34" S to 6° 52' 17" S. The National Park has an area of 120,551 ha composed of 76,214 ha of land and 44,337 ha of the surrounding reefs and sea. Most reefs in the area are classified into fringing reef associated with seagrass meadows, white sandy beach, and mangrove stands along the shoreline. The shoreline of the area is shaped by the oceanographic dynamics of the surrounding sea, especially by wave energies. Since the area has high wave energy, it is a very good place to spot sunglint occurrence. Consequently, most benthic habitats information in this area are severely affected by sunglint, and thus this location is perfect for analysing the effect of sunglint on satellite-based benthic habitats identification. The exact location of the study area was the south west part of Panaitan Island near Kasuaris Bay (Fig. 1).

Quickbird image used in this study is stored in 16-bit package (the original dynamic range is 11-bit). It was delivered in 2A level of correction and was acquired on 15<sup>th</sup> August 2002. This image is owned by DigitalGlobe and was

obtained for free from Global Land Cover Facility (GLCF). The image has 2.88 m spatial resolution due to 14.7° off-nadir recording. According to Quickbird Imagery Product Guide [6], the corrections applied on product level 2A are dark pixel subtract, non-uniformity correction (detector-to-detector relative gain), non-responsive detector fill, and a conversion for absolute radiometry. Sensor corrections account for internal detector geometry, optical distortion, scan distortion, any line-rate variations, and registration of the panchromatic and multispectral bands. Geometric corrections remove spacecraft orbit position and attitude uncertainty, earth rotation and curvature, and panoramic distortion. As we did not integrate any field data into the image, geometric correction using GCP (Ground Control Point) was not applied.



Fig. 1 The location of study area within Ujung Kulon National Park. The exact location is show in red box

## III. METHODS

Before applying sunglint removal technique, several adjustments were made to the image. At first, Quickbird image was converted into TOA (Top of Atmosphere) spectral radiance. The unit of TOA spectral radiance is  $W/m^2 \text{ str } \mu m$ . The formula to convert DN to TOA spectral radiance is as follow [12]:

$$L_{\text{Pixel,Band}} = \text{absCalFactor}_{\text{Band}} \times q_{\text{Pixel,Band}} \dots (1)$$

$$L_{\lambda_{\text{Pixel,Band}}} = L_{\text{Pixel,Band}} / \Delta\lambda_{\text{Band}} \dots (2)$$

Where  $L_{\text{Pixel,Band}}$  is TOA band-integrated radiance image pixels ( $W/m^2 \text{ str}$ ),  $L_{\lambda_{\text{Pixel,Band}}}$  is TOA band-averaged spectral radiance image pixels ( $W/m^2 \text{ str } \mu m$ ),  $\Delta\lambda_{\text{Band}}$  is the effective bandwidth ( $\mu m$ ) for a given band,  $\text{absCalFactor}_{\text{Band}}$  is the absolute radiometric calibration factor ( $W/m^2 \text{ str count}$ ) for a given band, and  $q_{\text{Pixel,Band}}$  is radiometrically corrected image pixels (Quickbird DN values).



The value of *absCalFactor* (K) has been revised based on the ground truth measurement and analysis from Joint Agency Commercial Imagery Evaluation (JACIE) Team. However, the revised value is only available on the .IMD file of the image acquired after 6<sup>th</sup> June 2003 00:00 GMT. The image used in this study was recorded on 15<sup>th</sup> August 2002, and thus the K-revised value was not in the .IMD file. Therefore, the calibration factor values for TOA spectral radiance calculation were taken from the value given in Table 1 [12].

TABLE I  
K-REVISED VALUE FOR QUICKBIRD IMAGE RECORDED BEFORE 6<sup>TH</sup> JUNE 2003

Band	K-revised (W/m <sup>2</sup> str count)
Blue	1.60412 x 10 <sup>-2</sup>
Green	1.43847 x 10 <sup>-2</sup>
Red	1.26735 x 10 <sup>-2</sup>
NIR	1.54242 x 10 <sup>-2</sup>

TOA spectral radiance image was still affected by atmospheric disturbance and the objects spectral signature was also still altered. As a resolve, FLAASH atmospheric correction module was applied. The basic data needed to run FLAASH module were the scene center location, sensor type, sensor altitude, average ground elevation, spatial resolution, the time of image acquisition, atmospheric model, aerosol model, and initial visibility. Some parameters were available directly on image metadata and others were derived from the analysis of geographical condition of the study area. Digital Elevation Model (DEM) data from SRTM image was used to estimate the average ground elevation of the study area. We put maritime aerosol model and tropical atmospheric model as other inputs. For the initial visibility, we used 40 km as the default for the visibility during clear sunny cloudless day. Finally, FLAASH processed those parameters to normalize atmospheric disturbances and repair the object's spectral signatures.

Sunglint removal was performed on atmospherically corrected image using the technique developed by [11]. This method utilizes IR band, which has similar index of refraction with visible bands, to remove the sunglint on visible bands. There are two assumptions used in this method, first, IR band produces minimum reflectance on the interaction with water body, and thus any NIR reflectance above that minimum value was considered as the offset caused by sunglint, assuming the water is optically deep. Second, the lowest IR value was the sunglint-free pixel. Afterward, to remove sunglint from visible bands, empirical model between IR band and visible bands were created to obtain data on how much sunglint affect the reflectance of optically deep water in NIR band. Finally, the additive sunglint value in IR band was integrated with the gradient of calibration obtained during the empirical model to remove sunglint in visible bands.

Basically, during the empirical model, this method requires the best IR band to be paired with the visible bands. The selection of the best IR band can be conducted by empirically connect each IR band with the visible bands to find the IR band that has the best fit with the visible bands. However, since Quickbird has only one IR band, the selection of the best IR band was not necessary. The empirical model between NIR band and visible bands was intended to obtain the gradient of calibration or slope (*b*) of various sunglint intensities occurred on both visible and NIR bands. Then, the slope (*b*) was used as the coefficient to perform sunglint correction on visible bands using the following equation:

$$Ri' = Ri - (bi \times (R_{NIR} - Min_{NIR})) \dots (3)$$

Where:

- Ri' : Sunglint-free reflectance
- Ri : Reflectance from visible band i
- bi : Regression slope (*b*)
- R<sub>NIR</sub> : Reflectance from NIR band
- Min<sub>NIR</sub> : Minimum NIR band/sunglint-free

To understand the effect of sunglint on altering the variation of spectra within particular benthic habitat class, COV analysis was used. The value of COV is unitless where bigger COV means greater variation and vice versa. Therefore, COV analysis may show the variation of the reflectance within particular habitat. This analysis was very useful because it showed the intra habitat spectra variation which conceptually should not be too high within a class. Theoretically, for any particular habitat class, COV value should stay low in order to avoid any confusion and misclassification during visual interpretation or digital classification.

COV value was calculated by rationing the standard deviation ( $\sigma$ ) to its mean ( $\mu$ ). The calculation of COV was conducted on each available habitat class. In general, benthic habitats in the study area consist of coral reefs, sparse and dense seagrass beds, and sand distributed at various depths. Last, in order to see how much sunglint alter the spectral variation of particular habitat class, the ratio of COV of each habitat class from uncorrected and sunglint-free image were calculated.

#### IV. RESULTS AND DISCUSSION

The conversion to TOA spectral radiance converted the unitless DN into energy unit of W/m<sup>2</sup> str  $\mu$ m. This unit was converted into  $\mu$ W/cm<sup>2</sup> str nm before performing atmospheric correction. Next, by using several FLAASH input parameters described previously, atmospherically corrected Quickbird image was obtained. Additionally, to check whether the correction was successful or not, spectral signatures of some

major objects were analysed and plotted. If the image has been successfully corrected, all objects should have proper spectral signature. For example, when green vegetation spectra are analysed, it will show a low reflectance in blue and red band but produce a high reflectance in green and NIR band. From the analysis, the spectral signatures for most known objects such as dry sand, green vegetation, and water body were correctly represented. Thus, we assumed that the atmospheric correction was successful. Figure 2 shows spectral signatures comparison between TOA spectral radiance image and atmospherically corrected image.

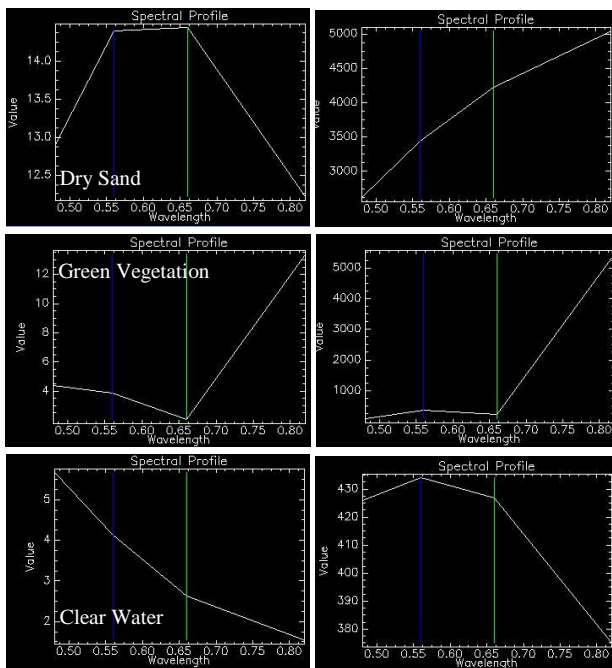


Fig.2 Spectral signatures comparison between TOA spectral radiance image (left) and atmospherically corrected image (right)

Atmospherically corrected image was processed for sunglint removal. First, the lowest NIR value was selected from optically deep water. This minimum NIR value was treated as the value of sunglint-free water. To obtain the minimum NIR value, pixels from various levels of sunglint intensities were selected. Three classes of different sunglint intensities covering low, medium, and high intensity were selected. However, from 25,600 selected optically deep water pixels, some negative values were found due to the residual error from atmospheric correction. Negative value posed a problem to the regression process since it did not provide valid data for the correction. Therefore, we decided to take the mean of the optically deep water pixels as the minimum NIR value. The average value of optically deep of NIR band water was 133.2.

To derive the slope for sunglint correction, 5,000 pixels with different sunglint intensities from each of VNIR bands were collected. Those pixels were put into bi-plot for creating linear regression between NIR band and visible bands. The regression analysis showed that the relationship between visible bands and NIR band was very high. All  $R^2$  (coefficient of determinant) between visible bands and NIR band exceeded 0.85. The results of linear regression for each bi-plot are shown in Figure 3.

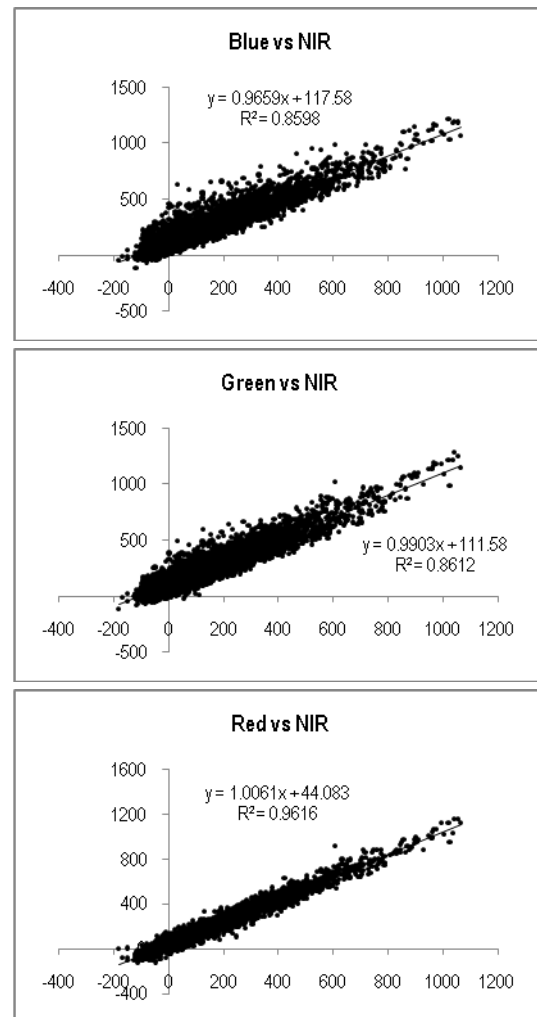


Fig. 3 Bi-plot of pixels with different sunglint intensity between visible bands and NIR band

TABLE III  
 THE  $R^2$  AND SLOPE (B) FOR THE REGRESSION ANALYSIS BETWEEN VISIBLE  
 BANDS AND NIR BAND

Bands	$R^2$	$b$
Blue – NIR	0.859	0.9659
Green – NIR	0.861	0.9903
Red - NIR	0.961	1.0061

Sunglint removal process was carried out using custom formula document on UNESCO Bilko 3.3 software. The data output was set to 32-bit floating point to accommodate decimals and negative values. Masking of the land pixels prior to sunglint removal was not performed since they will automatically be invalid after sunglint removal. Therefore, land masking process can be done afterward when performing further underwater image processing routines such as water column correction ([5], [20], [16], [24]) and PCA model ([3], [9], [17]). Then, the values of slope (Table 2) and minimum NIR were entered into Equation 3 to remove sunglint from the image. After the algorithm was applied, sunglint occurred on the water surface were effectively removed from the image. The comparison between the original image and sunglint-free image is shown in Figure 4.

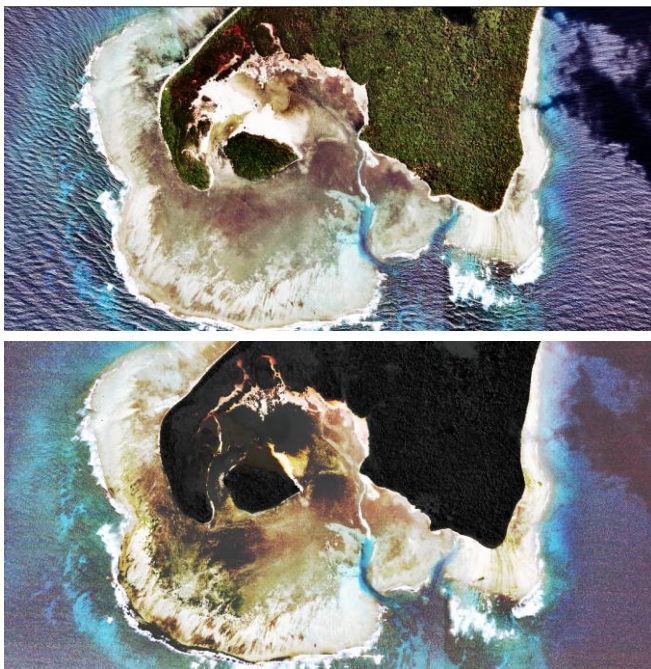


Fig. 4 Quickbird image before sunglint removal (above) and after sunglint removal (bottom)

The most obvious improvement that can be identified on sunglint-free image compared to the original image was the visual appearance of the objects located underwater. In the sunglint-free image, benthic habitats were clearly identified,

and information on areas that previously affected by sunglint has been revealed. Furthermore, the contrast between habitats which were not highly distorted by sunglint in the original image was also enhanced. For example, the contrast between seagrass habitat and sand habitat in the lagoon area was strongly enhanced. Moreover, the intra-variation within seagrass habitat was also increased, which is shown by higher visual variations on seagrass area. Conceptually, sunglint-free image has much better discriminating power, and thus it should be able to produce better benthic habitat map.

However, there were still several issues that should be carefully considered when using this sunglint-free image for underwater mapping process. First, if the sensor only has one IR band, the IR band itself cannot be corrected. However, NIR band is of limited usage for underwater mapping due to its poor ability to penetrate water. Second, as previously mentioned, the value of any terrestrial or emergent objects will be invalid after sunglint removal process. Figure 4 reveals that terrestrial objects such as dry sand, dry soil, and green vegetation were completely dark because their values are invalid. Thus, those objects should be masked out afterwards.

In fact, invalid value did not only apply on terrestrial objects but also on the emerging underwater objects. Underwater objects that were emerged due to the low tide at the time of image acquisition would also contain invalid value. Areas affected by the combination of sunglint and wave-breaking foams were not able to be resolved. Any information about benthic habitats located underlying this kind of water surface condition could not be recovered because there was no information to begin with. The aforementioned issues should be kept in mind and should not be ignored following the process of sunglint removal.

Visual appearance of the sunglint-free image was considered as its relative quality. As a result, concluding that sunglint-free image is better than the original one without any quantitative evident would be unfair and lack of confidence. It is because the ability and the agreement of each people to visually interpret remote sensing image varies greatly with the knowledge, experience, and educational background. Accordingly, to assess the image quantitatively, COV analysis on each class habitat was conducted.

COV analysis was conducted on each habitat class found on the image. The classification scheme consists of shallow sand, deep sand, dense seagrass, sparse seagrass, coral reef, and optically deep water. For each habitat class, 150 representative pixels were selected. Due to the existence of water column energy attenuation, habitat descriptor such as dense, sparse, deep, and shallow was qualitatively incorporated into each habitat class to obtain better understanding on COV result. Without water column correction, similar habitat distributed at different depths surely produces high COV due to the attenuation of light by water

column. Therefore, it was important to categorize those habitats based on their depth distribution. The result of COV analysis including the percentages of sunglint disturbance and the revealed additional information is shown in Table 3.

TABLE IIIII  
RESULTS OF COV ANALYSIS FOR EACH HABITAT CLASS

Habitat	Band	Raw Image	Corrected Image	Ratio COV (%)	Mean (%)	Sunglint Influence (%)
Optically Deep Water	#1 (Blue)	0.724	0.190	26.36	25.93	74.07
	#2 (Green)	0.799	0.213	26.67		
	#3 (Red)	0.821	0.203	24.76		
Shallow Sand	#1 (Blue)	0.116	0.072	62.30	66.88	33.12
	#2 (Green)	0.097	0.065	67.62		
	#3 (Red)	0.116	0.082	70.72		
Deep Sand	#1 (Blue)	0.261	0.111	42.55	38.60	61.39
	#2 (Green)	0.297	0.095	32.14		
	#3 (Red)	0.464	0.191	41.13		
Dense Seagrass	#1 (Blue)	0.253	1.070	23.64	29.25	70.75
	#2 (Green)	0.126	0.447	28.18		
	#3 (Red)	0.092	0.256	35.93		
Sparse Seagrass	#1 (Blue)	0.092	0.146	63.38	68.83	31.17
	#2 (Green)	0.054	0.074	72.22		
	#3 (Red)	0.068	0.096	70.89		
Coral Reef	#1 (Blue)	2.325	0.235	10.11	11.37	88.63
	#2 (Green)	1.232	0.16	12.98		
	#3 (Red)	1.735	0.191	11.02		
Total	Sunglint Disturbance					64.30
	Information Revealed					50.96

As seen in Table 3, an average of 64.3% variations within particular habitat class was due to the sunglint. Furthermore, habitats located in deeper water were more affected. Deep sand class was more influenced by sunglint than the sand distributed on shallower water. Coral reefs habitat located on deeper water was also strongly affected by sunglint. Deeper habitats such as coral reefs, optically deep water, and deep sand has 88.63%, 74.07% and 61.39% sunglint disturbance respectively. In contrast, at shallower water, where the waves were milder, the distortion caused by sunglint was not as strong as in the deeper water. It was shown by shallow sand habitat class whose information was only affected by sunglint as much as 33.12%. The results showed that sunglint should be minimized prior to benthic mapping process, especially during biophysical modelling and digital classification. If sunglint correction is not performed, any particular habitat area can be classified into more than one class. Thus, habitat class which should not be there will appear.

Interestingly, the removal of sunglint did not only minimize the variance of particular habitat but also improving it. The improvement in the spectra variation occurred on dense and sparse seagrass class. Rather than experiencing a decrease in the variance, they experienced variance improvement about 31.17% and 70.75% for sparse and dense seagrass respectively (Table 3 - red highlighted columns). It means that 70.75% more information on dense seagrass habitat has been revealed after sunglint correction. If dense seagrass areas

located in the south part of the Island were carefully identified visually, there were some obvious differences between the original image and the corrected one. On the original image, dense seagrass appears pretty homogenous and there will be a big chance of this area to be classified into one class of dense seagrass. Conversely, the sunglint-free image showed that there are some variations in that area, not only dominated by dense seagrass, but also seagrass at various densities interleaving with sand habitat. It seems that the removal of sunglint has enhanced the contrast, color, and texture of some habitats which improves the discriminating ability of the image.

Finally, sunglint correction is also very important for other applications such as ecological parameter modelling that requires, for example, an accurate measurement of seagrass shoots density which is highly related with its standing crop and LAI [7]. In a nutshell, sunglint removal is very useful for minimizing intra-habitat variation due to sunglint as well as improving the discrimination power of the image by enhancing the contrast, color, and texture of some habitats.

## V. CONCLUSIONS

This study showed that sunglint in high spatial resolution image can be removed using NIR band to improve the radiometric quality of the image for further underwater image analysis. Quantitatively, about 64.3% variations within particular habitat class were due to the existence of sunglint in water surface. Moreover, objects located at deeper water were more affected by sunglint. In addition, sunglint removal also managed to enhance the precision of information on areas that seems to be homogenous. However, the value of emerging and terrestrial objects will be invalid after the correction and should be masked prior to further image analysis. To conclude, sunglint removal is very useful on minimizing intra-habitat spectra variation caused by sunglint and improving the discrimination ability of the image by providing more precise information on benthic habitats variations.

## ACKNOWLEDGMENT

The author would like to thank Global Land Cover Facility (GLCF) of University of Maryland, United States and also DigitalGlobe for the free Quickbird image of Ujung Kulon National Park, Banten Province, Indonesia.

## REFERENCES

- [1] A. Fornes, G. Basterretxea, A. Orfila, A. Jordi, A. Alvarez, and J. Tintore, "Mapping Posidonia oceanica from IKONOS," *Journal of Photogrammetry & Remote Sensing*, vol. 60, pp. 315–322, 2006.
- [2] C.A. Meyer, and R. Pu, "Seagrass resource assessment using remote sensing methods in St. Joseph Sound and Clearwater Harbor, Florida, USA," *Environ Monit Assess*, 2011.
- [3] D. Mishra, S. Narumalani, D. Rundquist, and M. Lawson, "Benthic Habitat Mapping in Tropical Marine Environments Using QuickBird



- Multispectral Data," *Photogrammetric Engineering & Remote Sensing*, vol. 72, pp. 1037-1048, 2006.
- [4] D.L.B. Jupp, "Background and extensions to depth of penetration (DOP) mapping in shallow coastal waters," in *Proc. of the Symposium on Remote Sensing of the Coastal Zone*, 1988, IV.2.1-IV.2.19.
- [5] D.R. Lyzenga, "Passive Remote-Sensing Techniques for Mapping Water Depth and Bottom Features," *Applied Optics*, vol. 17, pp. 379-383, 1978.
- [6] DigitalGlobe™, "Quickbird Imagery Product - Product Guide (Revision 4.7.1)," DigitalGlobe™, Inc., 2006.
- [7] E.P. Green, P.J. Mumby, A.J. Edwards, and C.D. Clark, *Remote Sensing Handbook for Tropical Coastal Management*. Coastal Management Sourcebooks 3. Paris: UNESCO, 2000.
- [8] Image Science and Analysis Laboratory, NASA-Johnson Space Center. (2010) The Gateway to Astronaut Photography of Earth. [Online]. Available: <http://eol.jsc.nasa.gov/newsletter/RedSeaReefs.htm> (accessed August 21<sup>st</sup> 2010 10:44:38).
- [9] J. Palapa, "Pengolahan Citra Digital CASI-Themap Untuk Identifikasi dan Pemetaan Terumbu karang (Coral Reef) di Pulau Harapan, Kepulauan Seribu DKI Jakarta," Bachelor thesis, Faculty of Geography Universitas Gadjah Mada, Yogyakarta, Indonesia, 2002.
- [10] J.A. Urbanski, A. Mazur, and U. Janas, "Object-oriented classification of QuickBird data for mapping seagrass spatial structure," *International Journal of Oceanography and Hydrobiology*, vol. 38(1), pp. 27-43, 2009.
- [11] J.D. Hedley, A.R. Harborne, and P.J. Mumby, "Simple and Robust Removal of Sunlight for Mapping Shallow-Water Benthos," *International Journal of Remote Sensing*, vol. 26(10), pp. 2107-2112, 2005.
- [12] Krause, K, "Radiometric Use of Quickbird Imagery. Technical Note," DigitalGlobe™, Inc., 2005.
- [13] L. Barille, M. Robin, N. Harin, A. Bargain, and P. Launeau, "Increase in seagrass distribution at Bourgneuf Bay (France) detected by spatial remote sensing," *Aquatic Botany*, vol. 92, pp. 185-194, 2010.
- [14] M.B. Lyons, S.R. Phinn, and C.M. Roelfsema, "Long term monitoring of seagrass distribution in Moreton Bay, Australia, from 1972-2010 using Landsat MSS, TM, ETM+," *Proc. IGARSS 2010*, 2010, pp. 5-8.
- [15] P. Capolsini, S. Andrefouet, C. Rion, and C. Payri, "A Comparison of Landsat ETM+, SPOT HRV, IKONOS, ASTER and airborne MASTER Data for Coral Reef Habitat Mapping in South Pacific Island," *Canadian Journal of Remote Sensing*, vol. 29 (2), pp. 187-200, 2003.
- [16] P. Wicaksono, "Integrated Model of Water Column Correction Technique for Improving Satellite-Based Benthic Habitat Mapping," M. Sc. Thesis, Faculty of Geography Universitas Gadjah Mada, Yogyakarta, Indonesia, 2010.
- [17] P. Wicaksono, and S.H. Murti, "Factor Loadings Analysis: Which band contributes more on coral reef health condition identification?," *Proc. of the 10<sup>th</sup> SEASC 2009*, 2009, pp. 166-171.
- [18] P.J. Mumby, and A.R. Harborne, "Development of a systematic classification scheme of marine habitats to facilitate regional management and mapping of Caribbean coral reefs," *Biol Conserv*, vol. 88, pp. 155-163, 1999.
- [19] P.J. Mumby, E.P. Green, A.J. Edwards, and C. D. Clark, "Measurement of seagrass standing crop using satellite and digital airborne remote sensing," *Marine Ecology Progress Series*, vol. 159, pp. 51-60, 1997.
- [20] P.N. Bierwirth, T.J. Lee, and R.V. Burne, "Shallow Sea-Floor Reflectance and Water Depth Derived by Unmixing Multispectral Imagery," *Photogrammetric Engineering and Remote Sensing*, vol. 59(3), pp. 331-338, 1993.
- [21] S. Andrefouet, P. Kramer, D. Torres-Pulliza, K. E. Joyce, E.J. Hochberg, R. Garza-Perez, R., et al., "Multi-site evaluation of IKONOS data for classification of tropical coral reef environments," *Remote Sensing of Environment*, vol. 88, pp. 128-143, 2003.
- [22] S. Kakuta, T.Hiramatsu, T.Mitani, Y. Numata, H. Yamano, and M. Aramaki, "Satellite-based mapping of coral reefs in East Asia, Micronesia and Melanesia regions," *Proc. ISPRS Vol. 38 part 8*, 2010, pp.534-537.
- [23] S. Phinn, C. Roelfsema, V. Brando, and J. Anstee, "Mapping seagrass species, cover and biomass in shallow waters: An assessment of satellite multi-spectral and airborne hyper-spectral imaging systems in Moreton Bay (Australia)," *Remote Sensing of Environment*, vol. 112, pp. 3413-3425, 2008.
- [24] T. Sagawa, T. Komatsu, E. Boisnier, K. Ben Mustapha, A. Hattour, N. Kosaka, and S. Miyazaki, "A new Application Method for Lyzenga's Optical Model," [Online]. Available: <http://www.ceg.ncl.ac.uk/rspoc2007/papers/188.pdf> (accessed July 30<sup>th</sup> 2008).
- [25] V. Pasqualini, C. Pergent-Martini, G. Pergent, M. Agreil, G. Skoufas, L. Sourbes, and A. Tsirika, "Use of SPOT 5 for mapping seagrasses: an application to Posidonia oceanica," *Remote Sensing of Environment*, vol. 94, pp. 39-45, 2005.

### Biography

Pramaditya Wicaksono is currently active as lecturer and researcher in the Department of Cartography and Remote Sensing, Faculty of Geography, Universitas Gadjah Mada, Indonesia. In addition, he is also the current General Research Assistant for ACIAR (Australian Center for International Agricultural Research) Fisheries research project in Indonesia. Currently, he is undergoing his Doctorate degree in remote sensing in Universitas Gadjah Mada Indonesia and Cologne University of Applied Sciences Germany under CNRD (Center for Natural Resources and Development) project. His research topics cover coastal habitat ecological mapping especially coral reefs, seagrass, and mangroves. Any research collaboration is highly welcomed.